Calculating Reversible Potentials for Pt−H and Pt−OH Bond Formation in Basic Solutions

Yu Cai and Alfred B. Anderson*

Department of Chemistry, Case Western Reserve University, Cleveland, Ohio 44106

Received: September 15, 2004; In Final Form: December 14, 2004

Two redox reactions on platinum electrodes in base, the formation of underpotential deposited hydrogen, forming a Pt−H bond, and the electro-oxidation of water, forming a Pt−OH bond, were studied by two methods. The first applies a linear relationship between reaction energy in solution and standard reversible potential, an approach recently used in this lab to predict the formation potential of the surface-bonded species. This method depends on the availability of accurate surface adsorption bond strengths from measurement or theory and can be applied in two formats, the empirical model and the linear correlation model. The second method treats the reaction within the so-called double-layer model where reactants and products on the surface are well defined and are experiencing the influence of the electrolyte. When this approach is used, two coordination shells of hydrogen bonded water molecules are found necessary to sufficiently stabilize the hydroxide ion in this model, unlike acid for which past work showed only one shell around the hydronium ion is needed. The calculated reversible potentials for both reactions by the empirical and linear correlation models are in good agreement with the experimental onset potentials observed in cyclic voltammetry measurements for Pt(111) surface electrodes when empirical or accurately calculated H, OH, and H_2O adsorption energies are used. The double layer models for these reactions also yield satisfactory results, and it is concluded that the models should be useful for studying electron-transfer reactions in base, as has already been done for forming Pt−H and Pt−OH in acid solution.

1. Introduction

Reactions in basic electrolytes may be expected to be different from comparable ones in acid. For example, hydrogen evolution is known to be significantly slower in basic solutions than in acidic solutions.[1] In base, a hydrogen atom is extracted from H_2O and an electron is added to form OH^-(aq), while in acid an electron is added to H_3O^+(aq) and a hydrogen atom is extracted from it. The latter reaction has been theoretically explored for platinum electrodes using high-level quantum mechanical calculations and a local reaction center model.[2,3] Potential-dependent transition states and their activation energies were found wherein proton and reductive electron transfer were coupled during reduction, and conversely, hydrogen atom transfer and oxidative electron transfer were coupled. The onset potential in acid for under potential deposited (upd) H on platinum electrodes and the reversible potentials for the hydrogen evolution reaction (HER) and hydrogen oxidation reaction (HOR) could also be calculated quite accurately with the model.[4,5] The local reaction center models included one coordination shell of water molecules around the hydronium ions, and a potential was added to the Hamiltonian in the form of a point charge representing a Madelung sum of potential contributions due to the cations and anions in the electrolyte.[2] This is a zeroth order model of the electrochemical double layer plus the bulk electrolyte and will be referred to as a double layer model. In this paper local reaction center double layer models are developed and demonstrated for reactions in base by calculating reversible potentials for onset upd H and OH-(ads) formation.

A second model for predicting reversible potentials for forming reaction intermediates uses a linear correlation model based on a linear relationship between reaction internal energy changes, ΔE, and reversible potentials, $U°$, in solution. By modifying the solution reaction energies with surface adsorption energies, it is possible to predict reversible potentials for forming intermediates bonded to the catalytic sites.

In this work two reactions in base are studied, the formation of upd H from water reduction,

$$\mathrm{Pt\cdots H_2O} + \mathrm{e^-}(U) \rightarrow \mathrm{Pt{-}H} + \mathrm{OH^-(aq)} \qquad (1)$$

and the formation of Pt−OH from water oxidation,

$$\mathrm{Pt{-}OH_2} + \mathrm{OH^-(aq)} \rightarrow \mathrm{Pt{-}OH} + \mathrm{H_2O} + \mathrm{e^-}(U) \qquad (2)$$

The underpotential deposition of hydrogen has received continuous attention in the electrochemical community because the formation of upd H is the first step of hydrogen evolution reaction (HER) and plays an important role in the mechanistic explanation of fuel cell anode reactions.[1,9] It has long been recognized that Pt−OH forms on platinum electrodes in base from the oxidation of H_2O or OH^-. This species causes the inhibition of O_2 reduction on Pt cathodes in fuel cells.[10−12] These two reactions in acid solution have been studied previously using the theory that is applied in this paper.[2−5]

Hydration models for the OH^- in aqueous solution are needed, and there have been experimental and theoretical studies relating to this in the past.[13−28] Cluster calculations have been used in treating aqueous solvation of OH^-.[14,16,17,22] Two cluster-based viewpoints have appeared in the literature. In the first, two supermolecules are formed, $(H_2O)_n$ and $OH^-(H_2O)_n$, and the energies of embedding each in a polarizable continuum,

* Corresponding author. E-mail: aba@po.cwru.edu. Telephone: 216 368 5044. Fax: 216 368 3006.

10.1021/jp0458102 CCC: $30.25
Published on Web 03/22/2005

representing the bulk solvent, are calculated and included in the reaction energy of eq 3.

$$OH^- (g) + (H_2O)_n (aq) \rightarrow OH^-(H_2O)_n (aq) \qquad (3)$$

Mejías and Lago calculated the hydration enthalpy of OH^- using DFT and the COSMO variation of the self-consistent reaction field (SCRF). The best value obtained for the largest cluster model was about −520 kJ/mol (5.39 eV).[14] Zhan et al. predicted the free energy change for eq 3 using SVPE, a fully polarized continuum model. They found best estimate values of −90.9 kcal/mol (3.94 eV), −101.4 kcal/mol (4.40 eV), −104.5 kcal/mol (4.53 eV) for $n = 4$, 8, 12, respectively.[17]

The second viewpoint does not take into account the bulk solvent contribution to the solvation energy.[16,22] The reference states for all species are gas phase.

$$OH^-(g) + nH_2O (g) \rightarrow OH^-(H_2O)_n(g) \qquad (4)$$

A 65.8 kcal/mol (2.85 eV) hydration enthalpy was calculated for a $OH^-(H_2O)_3$ cluster by Pliego et al.,[16] and 81.2 kcal/mol (3.52 eV) was found for a $OH^-(H_2O)_4$ cluster. Various of DFT functionals were used by Wei et al. to calculate the stabilization of OH^- in $OH^-(H_2O)_n$.[22] For $n = 3$, the values varied between 60 and 70 kcal/mol (2.60 ∼ 3.04 eV) for the different methods.

In other work, Masamura has shown in an ab initio MO study that for each n in $OH^-(H_2O)_n$ isomers, the most stable one has a structure with C_n symmetry.[20,21] Water molecules surround the hydroxide ion and directly interact with the O of the hydroxide ion by hydrogen bonding. Merrill and Webb used effective fragment potentials, a QM/MM approach, to describe the hydration of OH^- up to the second shell with H_2O and compared energies with experimental numbers for the gas-phase ions.[23] Turki and co-workers employed symmetry-adapted perturbation theory to analyze the three-body interactions in the clusters $OH^-(H_2O)_n$, $n = 2$, 3, 4, 10.[24,25] In a recent experimental study, Robertson et al. determined the number of water molecules in the primary hydration shell to be three for hydroxide ion in the gas phase.[26] They observed a pronounced change in the vibrational spectrum when the number of water molecules increased to four. Hermida-Ramon and Karlstrom applied a quantum mechanical-statistical method to a quantum chemically described hydroxyl ion surrounded by 89 classically described water molecules.[27] They found a highly ordered first hydration shell composed of two water molecules bonded to the oxygen atom and two water molecules linked to the hydrogen atom. Tuckerman and Parrinello, based on a molecular dynamics simulation with eight H_2O molecules, suggested that four water molecules contact directly to the hydroxide ion.[28] From the above it can be surmised that OH^- in solution could have three or four water molecules in direct contact with it when in solution.

In this work the $OH^-(H_2O)_6$ cluster, including the second hydration shell, is shown to be a suitable model for the double layer calculations. When the linear correlation model is used the choice of hydration model is not important, and in fact the energy of OH^- by itself could be used, but some calculations with hydration were performed to compare with the literature.

2. Computational Approach

The hybrid density functional B3LYP and second-order perturbation theory MP2 in Gaussian program[29] were employed in this study. An effective core potential and double-ζ valence orbital (LANL2DZ) basis set was used for Pt. For light elements O and H, 6-31+G** basis functions, with diffuse functions on O and polarization functions on O and H, gave qualitatively correct electron affinity for the OH group, as given in Table 1; larger basis sets did not improve the EA significantly for this work, and the 6-31+G** basis set was chosen because it allows faster calculations than the larger basis sets.

TABLE 1: Electron Affinity, EA, of Gas Phase OH Calculated by Different Methods[a]

Basis set	EA (eV), MP2	EA (eV), B3LYP
6-31g**	−0.164	−0.060
6-31+g**	1.662	1.753
6-31++g**	1.671	1.760
6−311g**	0.019	0.241
6-311+g**	1.641	1.769
6-311++g**	1.641	1.770

[a] The experimental value is 1.825 eV.[32]

3. Results and Discussion

3.1. Linear Correlation of Reversible Potentials and Reaction Energies. To test models in preparation for the double layer and to compare with literature results, $OH^-(H_2O)_n$ ($n =$ 2, 3, 4) molecular clusters were fully optimized by both MP2 and B3LYP. When the number of water molecules was two, the calculations indicated that, depending on methodology, there are two different stable water molecule orientations, as shown in Figure 1. The MP2 calculation made the cis conformation more stable, and the B3LYP calculation made the trans conformation more stable. However, the MP2 and B3LYP calculations converged to the same structure when more water molecules were included. The hydration energies were calculated by the formula

$$E_{sol} = E(OH^-(H_2O)_n) - E(OH^-) - nE(H_2O) \qquad (5)$$

Results are listed in Table 2. The pyramidal structures for $n = 3$ and 4 agree well with the previous theoretical predictions.[13,16−19]

Electrochemical measurements in basic solution are often reported with potential referenced to the reversible hydrogen electrode (RHE) rather than the standard hydrogen electrode (SHE). From the Nernst equation,

$$U = U^\circ - \frac{RT}{nF}\ln\frac{[red]}{[ox]} \qquad (6)$$

where U is the potential, U° is the standard reversible potential, R is the gas constant, T is temperature, n is the number of electrons transferred, F is the Faraday constant, and the concentrations are for the reduced and oxidized species. A measurement on the first scale is related to a measurement on the second by the equation

$$U_{SHE} = U_{RHE} - 0.0592\text{pH} \qquad (7)$$

Quantum mechanical calculations are carried out with electrons on the vacuum scale, and this is related to the SHE scale by

$$\varphi = (4.6 + U/\text{V})\text{eV} \qquad (8)$$

where φ is the thermodynamic work function of the electrode and 4.6 eV is the thermodynamic work function of the SHE.[30]

Reversible potentials were calculated based on reaction energies, E_r, using the equation of the linear model:[7]

$$U^\circ = (-E_r/\text{eV} + c)\ \text{V} \qquad (9)$$

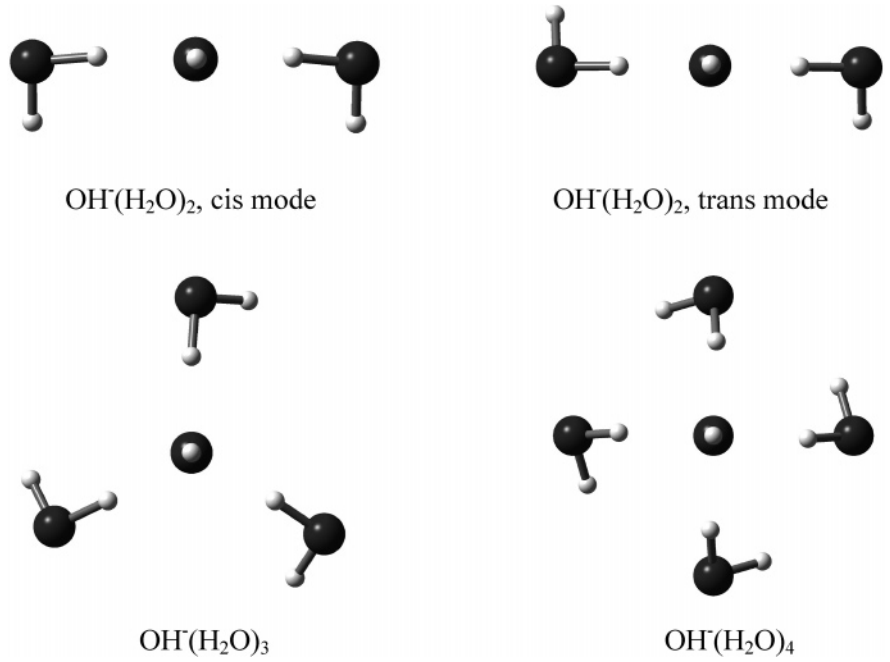

Figure 1. Calculated structures of the hydroxide ion when hydrated with using different numbers of water molecules. Big balls are oxygen atoms and smaller balls are hydrogen atoms.

TABLE 2: Hydroxide Anion Stabilization Energies, Δ*E*, Calculated Using Different Numbers of Water Molecules *N* in the First Hydration Shell

N	ΔE (eV), MP2	Δ*E* (eV), B3LYP
2	2.245	2.322
3	3.140	3.195
4	3.944	3.882

where the electron energy is 4.6 eV and the constant c is chosen by least-squares fitting of the calculated reaction energies to experimental reversible potentials using eq 9. If the reaction energies were exact, the constant c would correspond to the $\Delta H°$ and $T\Delta S°$ components of $\Delta G°$. When reaction energies are calculated with quantum theory, or estimated with standard bond strengths, and an approximate, but fixed, hydration model is used, the constant changes accordingly. In this section the hydronium cation and the hydroxyl anion had three water molecules coordinated to them. Thus the anion was $OH^-(H_2O)_3$ as shown in Figure 1, and the cation had the structure in previous publications.[3] The choice of the reference state of the water molecules involved in the hydration also affects the value of c. In this work the reference state is an isolated water molecule. Thus E_r is given by

$$E_r = (\sum_i \nu_i E(P_i) - \sum_j \nu_j E(R_j) - mE_{sol})/n \qquad (10)$$

where ν is the stoichiometric coefficients, E(P) and E(R) refer to the energy of the products and reactants respectively, m is the number of water molecules used for solvation, and E_{sol} is the solvation energy, which is defined for acid solutions as

$$E_{sol} = E(H_3O^+(H_2O)_3) - 4E(H_2O) \qquad (11)$$

and for basic solutions as

$$E_{sol} = E(OH^-(H_2O)_3) - E(OH^-) - 3E(H_2O) \qquad (12)$$

In the current model, vibrational zero point energies are not included because of near cancelation due to the conservation of the number of O−H bonds between reactant and product. It may be noted that a whole series of identical predictions in this section can be made when the hydroxyl anion is subjected to any other hydration model, including no hydration at all, or when any other water reference state model is used, because only the constant c in eq 9 changes and the linear relationship is otherwise unchanged.

Because a new basis set with a diffuse function on oxygen atoms was used in this study, we repeated the calculations in ref 7 using this basis set for the acid and base reactions. Reversible potentials for five reactions in acid solution, eqs 13−17, were used to determine the constant c for acid. The reactions were:

$$O_2(g) + 2H^+(aq) + 2e^- \rightarrow H_2O_2(aq)\ U° = 0.695\ V \qquad (13)$$

$$O_2(g) + 4H^+(aq) + 4e^- \rightarrow 2H_2O(aq)\ U° = 1.229\ V \qquad (14)$$

$$H_2O_2(aq) + 2H^+(aq) + 2e^- \rightarrow 2H_2O(aq)\ U° = 1.763\ V \qquad (15)$$

$$H_2O_2(aq) + H^+(aq) + e^- \rightarrow OH(g) + H_2O(aq)\ U° = 0.713\ V \qquad (16)$$

$$OH(g) + H^+(aq) + e^- \rightarrow H_2O(aq)\ U° = 2.813\ V \qquad (17)$$

Results, shown in Figure 2, are similar to past work. Data are in Table 3.

For base, four reactions were used:

$$O_2(g) + 2H_2O(aq) + 2e^- \rightarrow H_2O_2(aq) + 2OH^-(aq)\ U° = -0.146\ V \qquad (18)$$

$$O_2(g) + 2H_2O(aq) + 4e^- \rightarrow 4OH^-(aq)\ U° = 0.401\ V \qquad (19)$$

$$O_3(g) + H_2O(aq) + 2e^- \rightarrow O_2(g) + 2OH^-(aq)\ U° = 1.246\ V \qquad (20)$$

$$OH(g) + e^- \rightarrow OH^-(aq)\ U° = 1.984\ V \qquad (21)$$

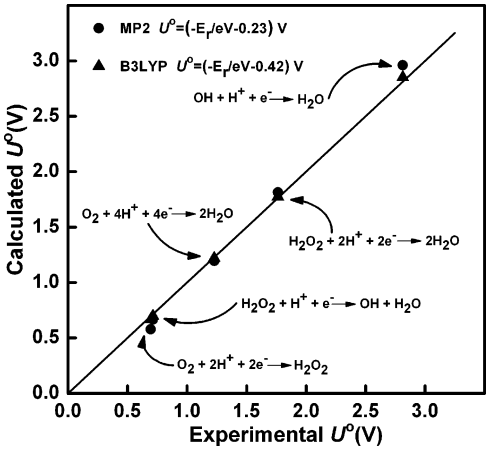

Figure 2. The comparison of calculated reversible potential, $U°$ according to the equations shown, where E_r is the reaction energy, and the experimental $U°$ for reduction reactions in acidic solution.

TABLE 3: Calculated Reversible Potentials, $U_{calc}°$, for Reduction Reactions in Acidic Solution[a]

	$U_{calc}°$ (V)		
reactions	MP2	B3LYP	U_{expt} (V)
$O_2(g) + 2H^+(aq) + 2e^- \rightarrow H_2O_2(aq)$	0.578	0.667	0.695
$O_2(g) + 4H^+(aq) + 4e^- \rightarrow 2H_2O(aq)$	1.196	1.221	1.229
$H_2O_2(aq) + 2H^+(aq) + 2e^- \rightarrow 2H_2O(aq)$	1.813	1.775	1.763
$H_2O_2(aq) + H^+(aq) + e^- \rightarrow OH(g) + H_2O(aq)$	0.666	0.699	0.713
$OH(g) + H^+(aq) + e^- \rightarrow H_2O(aq)$	2.961	2.851	2.813

[a] Experimental values U_{expt} from ref 31.

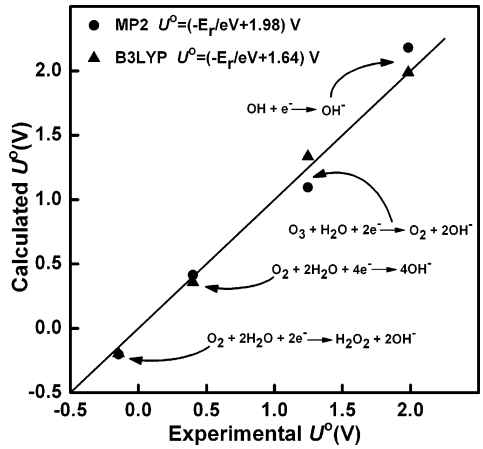

Figure 3. As in Figure 2 but for base.

The reversible potentials used in reactions 13−21 are taken from a compilation.[31] Some of them are connected to the values in acid by the Nernst equation.

The experimental EA of OH is 1.825 eV,[32] and the calculated EA of OH is 1.662 eV by MP2 and 1.753 eV by B3LYP. The added diffuse functions have made the calculated EA much more accurate than in the earlier study, where the calculated values were low by 1.988 eV for MP2 and 1.766 eV for B3LYP. The improved EA will be important to predicting reversible potentials in the double layer models of the next section and to future electron-transfer studies and activation energy determinations using the double layer models. The diffuse function on H was found to have a small effect on the description of the bond strengths, decreasing the Pt−H strength by 0.027 eV(B3LYP) or increasing it by 0.009 eV(MP2), and the Pt−OH bond strength was increased slightly, less than 0.01 eV, for both approaches. Results shown in Figure 3 are similar to those in ref 7.

3.2. Reversible Potentials for Forming Adsorbed Reaction Intermediates on Platinum: The Empirical and Linear Correlation Models. Equation 9 can be applied to predicting the reversible potentials for forming electrode surface intermediates by calculating the reaction energy and using the constant as determined above. The successes of this approach hinge on the $\Delta H°$ and $T\Delta S°$ components of $\Delta G°$ remaining the same, or sufficiently close, for the surface reaction. Success with acid reactions suggests this is true for them, and new results for base presented here will show comparable results for reactions in base.

An alternative use of the concept of eq 9 was demonstrated recently for water oxidation in acid.[8] In this approach, which can be conveniently called the empirical model, the potential for the surface reaction can be determined from the experimental standard solution value by adjusting the electron energy on the vacuum scale to take into account the adsorption energies of the reactants and products. The electron energy is then converted to the SHE scale with eq 8. This is a more transparent approach to estimate reversible potentials for forming surface intermediates during electrocatalytic reactions, and it allows the use of adsorption bond strengths from any source, including experimental determinations. Moreover, this method is independent of the linear relationship. Both methods will be used below.

Applying the empirical model for Pt−H formation in base it is assumed that H_2O is initially bonded to the Pt site:

$$\text{Pt- - -OH}_2 + e^-(U) \rightarrow \text{Pt−H} + \text{OH}^-(aq) \qquad (22)$$

The standard reversible potential for H· formation in acid is estimated to be −2.11 V[33] and in 0.1 M base it becomes −2.88 V. Increasing this by the experimentally determined Pt−H bond strength of 2.75 eV for low coverage[34] and decreasing it by the experimentally determined H_2O adsorption energy of 0.42 eV[35] yields a predicted reversible potential of −0.55 V for the onset of upd H in 0.1 M base. This is 0.13 V more negative than the observed low-coverage onset potential of about −0.42 V for the Pt(111) electrode surface in 0.1 M NaOH.[36−38] The adsorption bond strength of water at this potential, which is negative of the potential of zero charge, is not known but it should be somewhat less than the value for the uncharged surface because of a reduced water to Pt lone-pair donation interaction, possibly resulting in H_2O turning over to form weaker H···Pt hydrogen bonds. If this bond weakening were taken into account, the predicted reversible potential would be increased and might become closer to the −0.42 V experimental value. There are differences between the surfaces studied in refs 36 and 37. The (111) surface has a wide double layer region in base of ∼0.3 V and the (100) and (110) surface have narrow or vanishing double layer regions. The onset potentials for upd H on these surfaces are close to the (111) surface value of −0.42 V, being about −0.37 V for (100) and about −0.44 V for (110), based on our readings of figures in refs 36 and 37. All predicted reversible potentials for Pt−H and Pt−OH formation are in Table 5. The linear correlation model is not applicable with the constants shown in Figure 3 because the reaction

$$H_2O + e^- \rightarrow H + OH^- \qquad (23)$$

does not fit the linear correlation for the oxygen-containing reduction products. The experimental standard reversible potential is −2.94 V, and the calculated ones using the constants in the figure are −2.15 V and −2.61 V for the MP2 and B3LYP methods, respectively. However, as shown in the above

TABLE 4: Calculated Reversible Potentials, $U_{calc}°$, for the Reduction Reactions in Basic Solution[a]

reactions	$U_{calc}°$ (V) MP2	B3LYP	U_{expt} (V)
$O_2(g) + 2H_2O(aq) + 2e^- \rightarrow H_2O_2(aq) + 2OH^-(aq)$	−0.204	−0.196	−0.146
$O_2(g) + 2H_2O(aq) + 4e^- \rightarrow 4OH^-(aq)$	0.414	0.358	0.401
$O_3(g) + H_2O(aq) + 2e^- \rightarrow O_2(g) + 2OH^-(aq)$	1.094	1.336	1.246
$OH(g) + e^- \rightarrow OH^-(aq)$	2.179	1.988	1.984

[a] Experimental values U_{expt} are from ref 31.

TABLE 5: Predicted Onset Potentials from the Linear Correlation Model and Double Layer Model for Forming Pt−H and Pt−OH Bonds in 0.1 M Base[a]

	U_{emp}	U_{MP2}	U_{B3LYP}	U_{dl}	U_{expt}
Pt−H	−0.55	-	-	−0.65	−0.42
Pt−OH	−0.04	0.11	−0.09	−0.06	−0.12

[a] Results in the first column, U_{emp}, are from modifying $U°$ in these equations by empirical adsorption energies from the literature. U_{MP2} and U_{B3LYP} are from the reaction energies with the linear constant added as in eq 10 and Figure 3. U_{dl} is the reversible potential using double layer model, eqs 26 and 27. U_{expt} are taken from ref 36 for the Pt(111) electrode; see text for comparison with other surfaces.

paragraph, the empirical bond strength approach has greater generality and is applicable.

In applying the empirical model to Pt−OH formation in base the reaction is assumed to be

$$Pt{-}OH_2 + OH^- \rightarrow Pt{-}OH + H_2O + e^-(U) \qquad (24)$$

The standard reversible potential for OH formation is 1.984 V in base, the measured Pt−OH bond strength is about 2.5 eV at low coverage,[39,40] and using this and the experimental water adsorption energy in eq 24, the reversible potential in 0.1 M base is predicted to be −0.16 V. The experimental onset of Pt−OH formation on Pt(111) electrodes in 0.1 M base is ∼−0.12 V.[36] Thus the width of the double layer region is calculated to be 0.4 V vs the measured value of between 0.25 and 0.3 V for the Pt(111) electrode. In the case of the Pt(100) and (110) electrodes the reported double layer widths were near zero.[36,37] The formation of OH(ads) at potentials close to or less than the onset potential for upd H on the (100) and (110) surfaces has been attributed to defect sites on the platinum surface that bond OH more strongly.[37] In agreement with this, on Pt(111) a small number of defects created, scanning between −0.71 and 0.48 V, has been suggested to be forming OH(ads) at −0.29 V in 0.1 M NaOH.[38] Refining the model to take into account surface structure and double layer dependencies to explain the small differences in onset potentials for upd H and the large differences in OH(ads) onset potentials is a worthwhile goal for future model development.

In applying the linear relationship it is noted that the calculated Pt−OH bond strength is stronger than the reported low-coverage surface value by 0.48 eV for MP2 and 0.26 eV for B3LYP, and the Pt−OH_2 bond strength is weaker by 0.06 eV for MP2 and 0.09 eV for B3LYP. Taking this into account in the calculated reaction energies, the predicted MP2 and B3LYP reversible potentials, with respective values 0.11 V and −0.09 V, the latter being especially close to experimental value of ∼−0.12 V, might be anticipated from the fit in Figure 3. From these two calculations it can be seen that because of its good accuracy and greater computational speed, the B3LYP method was chosen for the base calculations with the double layer model, as discussed next.

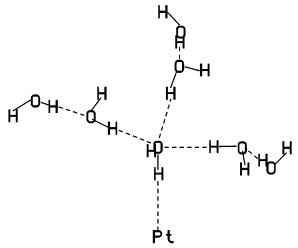

Figure 4. Structure of PtH reduction precursor Pt- - -$HOH(H_2O)_6$.

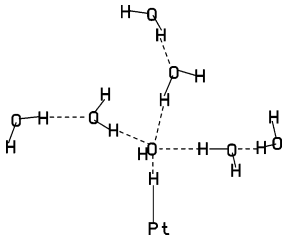

Figure 5. Structure of PtH oxidation precursor PtH- - -$OH^-(H_2O)_6$.

3.3. Reversible Potentials for Forming Adsorbed Reaction Intermediates on Platinum: The Double Layer Model. For the double layer model, it was found that three solvating waters are not enough to properly describe OH^- during electron transfer. An unexpected proton-transfer took place in the oxidation precursor:

$$Pt{-}H\text{- - -}OH^-(H_2O)_3 \rightarrow Pt^-\text{- - -}H_2O(H_2O)_3 \qquad (25)$$

This was understood in terms of the calculated proton affinities of Pt^-, 15.6 eV, and OH^-, 17.2 eV, which means that OH^- is more attractive to H^+ in this hydration model. Three second-shell hydrating water molecules were added to the first shell to stabilize the OH^-. The double layer reaction model is now

$$Pt\text{- - -}H_2O\text{- - -}(H_2O\text{- - -}H_2O)_3 + e^-(U) \rightarrow Pt{-}H\text{- - -}OH^-(H_2O\text{- - -}H_2O)_3 \qquad (26)$$

During the calculations, a point charge of $q = 1$ located 20 Å from the OH^- is added to the Hamiltonian to represent the potential contribution from evenly spaced +1 cations and −1 anions in a 0.1 M base, such as sodium hydroxide. The structure of the reduction precursor on the left in eq 26 is shown in Figure 4, and the structure of the oxidation precursor is in Figure 5. The optimization of the redox precursor structures was separated into two steps. First, a full optimization was done on the three water molecules in the first hydration shell, shown in Figure 1, and the 175° that was obtained for each O- - -H−O angle was subsequently used for the first and second hydration shell without reoptimization to reduce the number of variables and define simple models. The water H−O−H angles were also set equal and fixed in subsequent calculations as were the O−H distances. Then three more water molecules, each hydrogen-bonded to a water molecule in the first shell, were added to form the second hydration shell. When this was done the first shell water molecules around the OH^- were relaxed along the O- - -H axes and the O- - -H−O−H dihedral angles were optimized. In the second shell the three O- - -H distances were set equal and optimized as were the O- - -H−O−H dihedral angles. As in the first shell, the water H−O−H angles were also set equal and fixed in subsequent calculations as were the O−H distances. Thus, in summary, for hydration model optimizations, the water molecules were given rigid structures

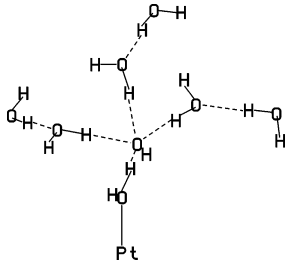

Figure 6. Structure of PtOH oxidation precursor $PtOH_2$- - -$OH^-(H_2O)_6$.

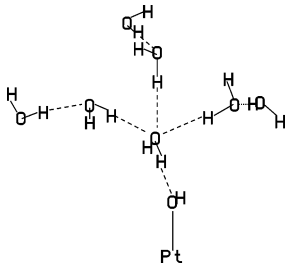

Figure 7. Structure of PtOH reduction precursor PtOH- - -$H_2O(H_2O)_6$.

and the rotational orientation of each water molecule was varied along with the hydrogen bond distances.

The oxidation precursor structure is affected by the charge of OH^- and the HO^-- - -HPt hydrogen bond distance is short at 1.115 Å and the OH and PtH each bear about 1/2 of the net −1 charge, meaning the charge is delocalized to be partially on the Pt. Taking into account the overestimation of the Pt−H bond strength, the calculated reversible potential $U°$ for this reaction is −0.65 V, which is 0.2 V more negative than experiment and 0.1 V more negative than the other predicted value for the onset of upd H on Pt(111) in 0.1 M NaOH. This predicted reversible potential would be affected by any corrections made for the H_2O−Pt hydrogen bond strength, which, at 0.33 eV, might be overestimated, and by any corrections that might be made to the electrolyte structure-dependent Madelung potential. However, this is expected to be a good working model for electron-transfer studies in acid electrolytes of the type done in refs 2−6 and 41.

The double-layer model for calculating the formation of Pt−OH is

$$\text{Pt- - -}OH_2\text{- - -}OH^- \text{ - - -}(H_2O\text{- - -}H_2O)_3 \rightarrow \text{Pt}-OH\text{- - -}H_2O\text{- - -}(H_2O\text{- - -}H_2O)_3 + e^-(U) \quad (27)$$

Calculations with this model were made in the same way as for Pt−H formation. Structures of the oxidation and reduction precursors are in Figures 6 and 7, respectively. The structure of the oxidation precursor is strongly affected by the charge on OH^-: the Pt−OH_2- - -OH^- hydrogen bond is very short at 1.168 Å, the O−H bond in the water molecule is long at 1.232 Å, and the charge is delocalized about −0.7 on OH and −0.3 on Pt.

Taking into account the overestimation of the Pt−OH bond strength relative to the low coverage surface value, the calculated reversible potential $U°$ is −0.06 V (Table 5). This is close to the other predicted values and to the experimental value of −0.12 V for the onset of surface OH formation on Pt(111) in 0.1 M NaOH. This should be a good working model for electron-transfer studies. According to ref 36, the reversible potentials for OH(ads) formation on the (100) and (110) surfaces are the same as the onset potentials for upd H formation, about −0.42 V and −0.32 V, respectively. Explaining the structure sensitivity of the experimental results will require further experimental work, or, in the case of theory, the use of large cluster models of the surfaces.

4. Conclusions

The observation of linear relationships between reversible potentials and reaction energies invites the creation of models for estimating changes in reversible potentials due to surface bonding. The empirical and linear correlation models presented here focus on electrode-intermediate bond strengths alone. The successes of the models, though results are only accurate to within ∼0.2 V, mean that the $\Delta H°$ and $T\Delta S°$ components of $\Delta G°$ are not affected by the presence of an interface by more than ∼0.2 eV per electron transferred for the reactions considered in this work. This helps understanding of why hydration energies can be ignored: for a given electron and proton transfer reaction they change by approximately the same amount whether an interface is involved. Interestingly, the reaction energy for the reduction of water to form hydrogen atoms in solution does not lie within the linear correlation that holds for the other reactions in base, and this means that the hydration energy difference when a hydrogen atom is formed is different from the other reactions. From the Nernst equation, the same will be true in acid electrolyte.

The double layer local reaction center model invokes the electrolyte, water molecules of hydration are included for the reduction precursor and the oxidation precursor, and their hydrogen bond distances are allowed to relax in response to changes in charge of the reaction centers. This model is different from the linear correlation model in that it includes the properties of the reaction center involved in the electron transfer in greater detail, contains enough information to define reaction coordinates, and can be used for studies of the electrode potential dependencies of electron-transfer reactions. Results for Pt−OH formation are good within this model when inaccuracies in Pt−OH bond strength relative to surface values are taken into account. The same is true for Pt−H bond formation. The double layer local reaction center models developed here can be used to calculate electrode potential dependence for the activation energies for upd H formation on Pt and Pt−OH formation using constrained variation theory, as has been done for forming these surface species in acid solution.[2−6,41]

Acknowledgment. This research is supported by the National Science Foundation, Grant. No. CHE-9982179.

References and Notes

(1) Barber, J. H.; Conway, B. E. *J. Electroanal. Chem.* **1999**, *461*, 80−89.

(2) Anderson, A. B.; Neshev, N. M.; Sidik, R. A.; Shiller, P. *Electrochim. Acta* **2002**, *47*, 2999−3008.

(3) Anderson, A. B.; Albu, T. V. *J. Electrochem. Soc.* **2000**, *147*, 4229−4238.

(4) Cai, Y.; Anderson, A. B. *J. Phys. Chem. B* **2004**, *108*, 9829−9833.

(5) Anderson, A. B.; Sidik, R. A.; Narayanasamy, J.; Shiller, P. *J. Phys. Chem. B* **2003**, *107*, 4618−4623.

(6) Anderson, A. B. *Electrochim. Acta* **2003**, *48*, 3743−3749.

(7) Anderson, A. B.; Narayanasamy, J. *J. Phys. Chem. B* **2003**, *107*, 6898−6901.

(8) Roques, J.; Anderson, A. B. *J. Electrochem. Soc.* **2004**, *151*, E85-E91.

(9) Conway, B. E.; Tilak, B. V. *Electrochim. Acta* **2002**, *47*, 3571−3594.

(10) Tarasevich, M. R.; Vilinskaya, V. S. *Elektrokhimiya* **1973**, *9*, 98−101.

(11) Adzic, R. R. *Structural Effects in Electrocatalysis and Oxygen Electrochemistry*; Pennington: The Electrochem. Soc. Inc., 1992; 92-11, p 419.

(12) Uribe, F. A.; Wilson, M. S.; Springer, T. E.; Gottesfeld, S. *Structural Effects in Electrocatalysis and Oxygen Electrochemistry*; Pennington: The Electrochem. Soc. Inc., 1992; 92-11, p 494.
(13) Vegiri, A.; Shevkunov, S. V. *J. Chem. Phys.* **2000**, *113*, 8521−8530.
(14) Mejías, J. A.; Lago, S. *J. Chem. Phys.* **2000**, *113*, 7306−7316.
(15) Weck, G.; Milet, A.; Moszynski, R.; Kochanski, E. *J. Phys. Chem. A* **2002**, *106*, 12084−12094.
(16) Pliego, J. R.; Riveros, J. M. *J. Chem. Phys.* **2000**, *112*, 4045−4052.
(17) Zhan, C.; Dixon, D. A. *J. Phys. Chem. A* **2002**, *106*, 9737−9744.
(18) Tuñón, I.; Rinaldi, D.; Ruiz-López, M. F.; Rivail, J. L. *J. Phys. Chem.* **1995**, *99*, 3798−3805.
(19) Xantheas, S. *J. Am. Chem. Soc.* **1995**, *117*, 10373−10380.
(20) Masamura, M. *J. Mol. Struct. (THEOCHEM)* **2000**, *498*, 87−91.
(21) Masamura, M. *J. Chem. Phys.* **2002**, *117*, 5257−5263.
(22) Wei, D.; Proynov, E. I.; Milet, A.; Salahub, D. R. *J. Phys. Chem. A* **2000**, *104*, 2384−2395.
(23) Merrill, G. N.; Webb, S. P. *J. Phys. Chem. A* **2003**, *107*, 7852−7860.
(24) Turki, N.; Milet, A.; Rahmouni, A.; Ouamerali, O.; Moszynski, R.; Kochanski, E.; Wormer, P. E. S. *J. Chem. Phys.* **1998**, *109*, 7157−7168.
(25) Turki, N.; Milet, A.; Ouamerali, O.; Moszynski, R.; Kochanski, E. *J. Mol. Struct. (THEOCHEM)* **2002**, *577*, 239−253.
(26) Robertson, W. H.; Diken, E. G.; Price, E. A.; Shin, J.; Johnson, M. A. *Science* **2003**, *299*, 1367−1372.
(27) Hermida-Ramon, J. M.; Karlstrom, G. *J. Phys. Chem. A* **2003**, *107*, 5217−5222.
(28) Tuckerman M. E.; Marx D.; Parrinello M. *Nature* **2002**, *417*, 925−929.
(29) Frisch, M. J.; Trucks, G. W.; Schlegel, H. B.; Scuseria, G. E.; Robb, M. A.; Cheeseman, J. R.; Montgomery, J. A., Jr.; Vreven, T.; Kudin, K. N.; Burant, J. C.; Millam, J. M.; Iyengar, S. S.; Tomasi, J.; Barone, V.; Mennucci, B.; Cossi, M.; Scalmani, G.; Rega, N.; Petersson, G. A.; Nakatsuji, H.; Hada, M.; Ehara, M.; Toyota, K.; Fukuda, R.; Hasegawa, J.; Ishida, M.; Nakajima, T.; Honda, Y.; Kitao, O.; Nakai, H.; Klene, M.; Li, X.; Knox, J. E.; Hratchian, H. P.; Cross, J. B.; Adamo, C.; Jaramillo, J.; Gomperts, R.; Stratmann, R. E.; Yazyev, O.; Austin, A. J.; Cammi, R.; Pomelli, C.; Ochterski, J. W.; Ayala, P. Y.; Morokuma, K.; Voth, G. A.; Salvador, P.; Dannenberg, J. J.; Zakrzewski, V. G.; Dapprich, S.; Daniels, A. D.; Strain, M. C.; Farkas, O.; Malick, D. K.; Rabuck, A. D.; Raghavachari, K.; Foresman, J. B.; Ortiz, J. V.; Cui, Q.; Baboul, A. G.; Clifford, S.; Cioslowski, J.; Stefanov, B. B.; Liu, G.; Liashenko, A.; Piskorz, P.; Komaromi, I.; Martin, R. L.; Fox, D. J.; Keith, T.; Al-Laham, M. A.; Peng, C. Y.; Nanayakkara, A.; Challacombe, M.; Gill, P. M. W.; Johnson, B.; Chen, W.; Wong, M. W.; Gonzalez, C.; Pople, J. A. *Gaussian 03*, revision B.04; Gaussian, Inc.: Pittsburgh, PA, 2003.
(30) Bockris, J. O. M.; Khan, S. U. M. *Surface Electrochemistry*; Plenum Press: New York, 1993; p 493.
(31) Bard, A. J.; Parsons, R.; Jordan, J. *Standard Potentials in Aqueous Solution*; Marcel Dekker Inc.: New York and Basel, 1985.
(32) Huber, K. P.; Herzberg, G. *Molecular Spectra and Molecular Structure, Vol IV, Constants of Diatomic Molecules*; van Nostrand Reinhold: New York, 1979; p 516.
(33) Anderson, A. B.; Kang, D. B. *J. Phys. Chem. A* **1998**, *102*, 5993−5996.
(34) Christman, K. *Electrocatalysis*; Lipkowski, J., Ross, P. N., Eds.; Wiley: New York, 1998; p 1.
(35) Sexton, B. A.; Hughes, A. E. *Surf. Sci.* **1984**, *140*, 227−248.
(36) Schmidt, T. J.; Ross, P. N.; Markovic, N. M. *J. Electroanal. Chem.* **2002**, *524*−*525*, 252−260.
(37) Schmidt, T. J.; Ross, P. N.; Markovic, N. M. *J. Phys. Chem. B* **2001**, *105*, 12082−12086.
(38) Spendelow, J. S.; Lu, G. Q.; Kenis, P. J. A.; Wieckowski, A. *J. Electroanal. Chem.* **2004**, *568*, 215−224.
(39) Mooney, C. E.; Anderson, L. C.; Lunsford, J. H. *J. Phys. Chem.* **1993**, *97*, 2505−2506.
(40) Markovic, N. M.; Schmidt, T. J.; Grgur, B. N.; Gasteiger, H. A.; Behm, R. J.; Ross, P. N. *J. Phys. Chem. B* **1999**, *103*, 8568−8577.
(41) Kostadinov, L. N.; Anderson, A. B. *Electrochem. Solid State Lett.* **2003**, *6*, E30−E33.